

A Unified Solution to Diverse Heterogeneities in One-Shot Federated Learning

Jun Bai*

McGill University
Montreal, Canada
jun.bai@mcgill.ca

Yiliao Song*

The University of Adelaide
Adelaide, Australia
lia.song@adelaide.edu.au

Di Wu*

University of Southern Queensland
Toowoomba, Australia
di.wu@unisq.edu.au

Atul Sajjanhar

Deakin University
Melbourne, Australia
atul.sajjanhar@deakin.edu.au

Yong Xiang

Deakin University
Melbourne, Australia
yong.xiang@deakin.edu.au

Wei Zhou

Monash University
Melbourne, Australia
wei.zhou2@monash.edu

Xiaohui Tao

University of Southern Queensland
Toowoomba, Australia
xiaohui.tao@unisq.edu.au

Yan Li

University of Southern Queensland
Toowoomba, Australia
yan.li@unisq.edu.au

Yue Li

McGill University
Montreal, Canada
yueli@cs.mcgill.ca

Abstract

One-Shot Federated Learning (OSFL) restricts communication between the server and clients to a single round, significantly reducing communication costs and minimizing privacy leakage risks compared to traditional Federated Learning (FL), which requires multiple rounds of communication. However, existing OSFL frameworks remain vulnerable to distributional heterogeneity, as they primarily focus on model heterogeneity while neglecting data heterogeneity. To bridge this gap, we propose FedHydra, a unified, data-free, OSFL framework designed to effectively address both model and data heterogeneity. Unlike existing OSFL approaches, FedHydra introduces a novel two-stage learning mechanism. Specifically, it incorporates model stratification and heterogeneity-aware stratified aggregation to mitigate the challenges posed by both model and data heterogeneity. By this design, the data and model heterogeneity issues are simultaneously monitored from different aspects during learning. Consequently, FedHydra can effectively mitigate both issues by minimizing their inherent conflicts. We compared FedHydra with five SOTA baselines on four benchmark datasets. Experimental results show that our method outperforms the previous OSFL methods in both homogeneous and heterogeneous settings. Our code is available at <https://anonymous.4open.science/r/Fed-SA-A4D7>.

CCS Concepts

• **Computing methodologies** → **Distributed artificial intelligence.**

Keywords

One-Shot Federated Learning, Data Free, Heterogeneity Problems

1 Introduction

Federated Learning (FL) can promise enhanced privacy and data security via collaborative effort in training a global model across multiple clients without sharing private data [22]. Existing studies implicate two *limitations* in traditional FL, *i.e.*, **(I)** it is vulnerable to

potential attacks due to its reliance on multi-round communications [13, 28, 35, 40]; **(II)** the performance will be largely impaired under heterogeneity scenarios [1, 12, 14, 23]. These issues highlight the need for heterogeneity-tolerant and short-communicated FLs to ensure privacy and efficiency across diverse applications.

One-Shot Federated Learning (OSFL) is proposed to overcome *limitation (I)* by restricting communication to a single round, where all clients are assumed to participate and upload their locally converged models to the server at once [7]. By this design, OSFL can minimize risks associated with data sharing and communication costs while maintaining data privacy. Meanwhile, existing OSFL shows potential capabilities to address *limitation (II)* [6, 7, 10, 18, 39, 42]. For example, recent methods have used auxiliary public datasets [6, 7, 18, 42] or embedding client data [10] to mitigate the heterogeneity issue. Despite its potential, OSFL still performs poorly in highly heterogeneous scenarios, which largely prevents OSFL from being applied in reality [12, 23, 26, 33, 43].

To further discover the cause for low heterogeneity tolerance in existing OSFLs, we review the heterogeneity scenarios from *data* or *model* dimensions. *Data heterogeneity* can be presented as label heterogeneity *i.e.*, Fig. 1 (a), which arises when clients have different classes [9] or size heterogeneity *i.e.*, Fig. 1 (b), which refers to the disparity in dataset volumes across clients [8]. The label heterogeneity can skew global model performance towards more prevalent classes, while size heterogeneity leads to the problem of dominance by larger datasets. *Model heterogeneity i.e.*, Fig. 1 (c) involves clients employing diverse model architectures [19].

Diverse heterogeneity scenarios often coexist, yet existing solutions typically address only one dimension. Methods using auxiliary public datasets mitigate data heterogeneity [6, 7, 18, 42] but fail to handle model heterogeneity, limiting their applicability to customized models. To eliminate the need for auxiliary datasets and support model heterogeneity, knowledge distillation-based methods like DENSE [39] have been proposed. Co-Boosting [5], an extension of DENSE, enhances synthetic data and ensemble models through adversarial sample generation and dynamic client weighting but still struggles with severe data heterogeneity. Besides, aggregation-based

*Authors contributed equally to this research.

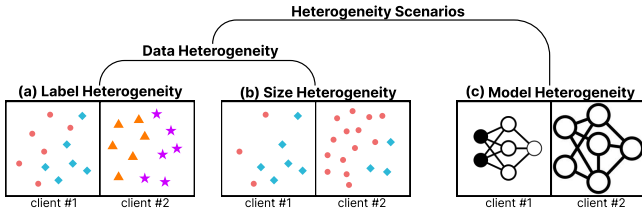


Figure 1: Illustration of heterogeneity problems (a) Label Heterogeneity, (b) Size Heterogeneity, and (c) Model Heterogeneity.

approaches like OT [31] facilitate one-shot knowledge transfer by aligning and merging model parameters without retraining. However, data heterogeneity remains a major challenge, weakening their performance. These limitations underscore the need for a holistic approach that addresses both data and model heterogeneity in OSFL.

Existing methods [6, 39] fail to effectively assess the capability of different clients in handling heterogeneity when aggregating heterogeneous client models on the server. Therefore, they do not adequately address data heterogeneity. Since data heterogeneity originates from clients, its impact first propagates through the client before reaching the server. To mimic this client-server pathway, we propose FedHydra, which operates in two stages. In the *Model Stratification (MS)* stage, FedHydra evaluates each client model’s classification capability across all class labels, enabling Stratified Aggregation (*SA*) for heterogeneous client models. Additionally, in the *Heterogeneity-Aware Stratified Aggregation (HASA)* stage, FedHydra further enhances robustness against both data and model heterogeneity through refined *SA*. With this design, FedHydra effectively mitigates data and model heterogeneity issues by minimizing their inherent conflicts, leading to a more stable and efficient OSFL.

The contributions of the proposed FedHydra are as follows: 1) A *Model Stratification* stage is introduced to assess client models’ classification capability across class labels, establishing the foundation for stratified aggregation on heterogeneous client models. 2) A *Heterogeneity-Aware Stratified Aggregation* stage is designed to tackle both data and model heterogeneity in OSFL through a data-free, stratified aggregation-guided distillation framework. 3) Extensive evaluations on multiple benchmark datasets under both homogeneous and heterogeneous settings consistently demonstrate FedHydra’s superior efficacy over SOTA baselines.

2 Related Works

FL [22], a decentralized framework, faces challenges from heterogeneity. Strategies to address this include FedAvg [22] enhancements with proximal terms [1, 14, 17, 19, 31, 34] and knowledge distillation (KD) to mitigate parameter averaging issues using auxiliary data [20, 29] or generative models [41, 43]. Recent efforts optimize client selection [32], prevent catastrophic forgetting [12], and enhance model adaptability [23]. However, these methods rely on repeated communications, making them unsuitable for OSFL.

OSFL offers efficient learning with minimal communication, employing heuristic client selection and KD with auxiliary datasets for aggregation [7]. Later research expanded KD to diverse model structures [18], but reliance on auxiliary data limits applicability where data sharing is restricted. Secure data transfer methods, including

dataset distillation [42] and data augmentation [30], have been explored. Dense [39] and Co-Boosting [5] introduced data-free KD using a generator trained on client model ensembles. Heinbaugh et al. [10] proposed FEDCVAE-ENS and FEDCVAE-KD for tackling statistical heterogeneity via KD but require local data manipulation, posing data leakage risks. However, many OSFL methods struggle with or remain untested against high statistical heterogeneity, a gap our approach aims to address.

In data-free KD [21], DeepInversion [37] optimizes RGB pixels using cross-entropy and batch normalization losses, while DAFL [3] employs a generator with the teacher model as a discriminator. ZSKT [24] generates images to highlight student-teacher discrepancies, reducing overfitting. Unlike methods selecting optimal images for KD, our approach leverages all generated intermediates to mitigate overfitting risks. While Raikward et al. [27] use random noise for KD, their method still relies on real images. In contrast, our strategy enables OSFL without real images.

3 Methodology

3.1 FedHydra: An overview

The proposed FedHydra framework introduces a data-free OSFL training scheme with two key stages: **MS** and **HASA**. **HASA** further comprises two phases: data generation and model distillation. Following the standard OSFL process, all clients transmit their converged local models to the server in a single communication round, where the core implementation of FedHydra takes place.

Specifically, in **MS**, we assess client models’ classification capabilities across class labels based on generator training loss guided by local models, aiming to refine aggregation weights. These refined aggregation weights inform *SA* for client prediction logits, facilitating both generator and global model training. In **HASA**, data generation trains a generator using *SA*-based client guidance, producing synthetic data for global model distillation. The two phases alternate, aligning knowledge between synthetic and real data. It is important to note that the designed generator serves different roles in the two stages: it assists in evaluation during **MS** and generates synthetic data during the aggregation process. Finally, the server constructs a unified global model from client models in a single communication round. The learning process is depicted in Fig. 2, with Algorithm 1 detailing the full training procedure.

3.2 Model Stratification

We first perform **MS** to assess the classification capabilities of all uploaded converged client models across all class labels using an auxiliary generator model. Specifically, we need to obtain two relative weight matrices. One weight matrix represents the guidance capability of a particular client model across all class labels, and the other represents the guidance capability for a particular class label across all client models.

Assume there are c class labels indexed by j and m clients indexed by k in the federated task. To evaluate the classification capability of one client model for a particular class j , we can allow a single client model $F_k(\theta^k)$ to separately guide the training of the Generator $G(\theta_G)$ for generating data with the same class label. In the t^{th}

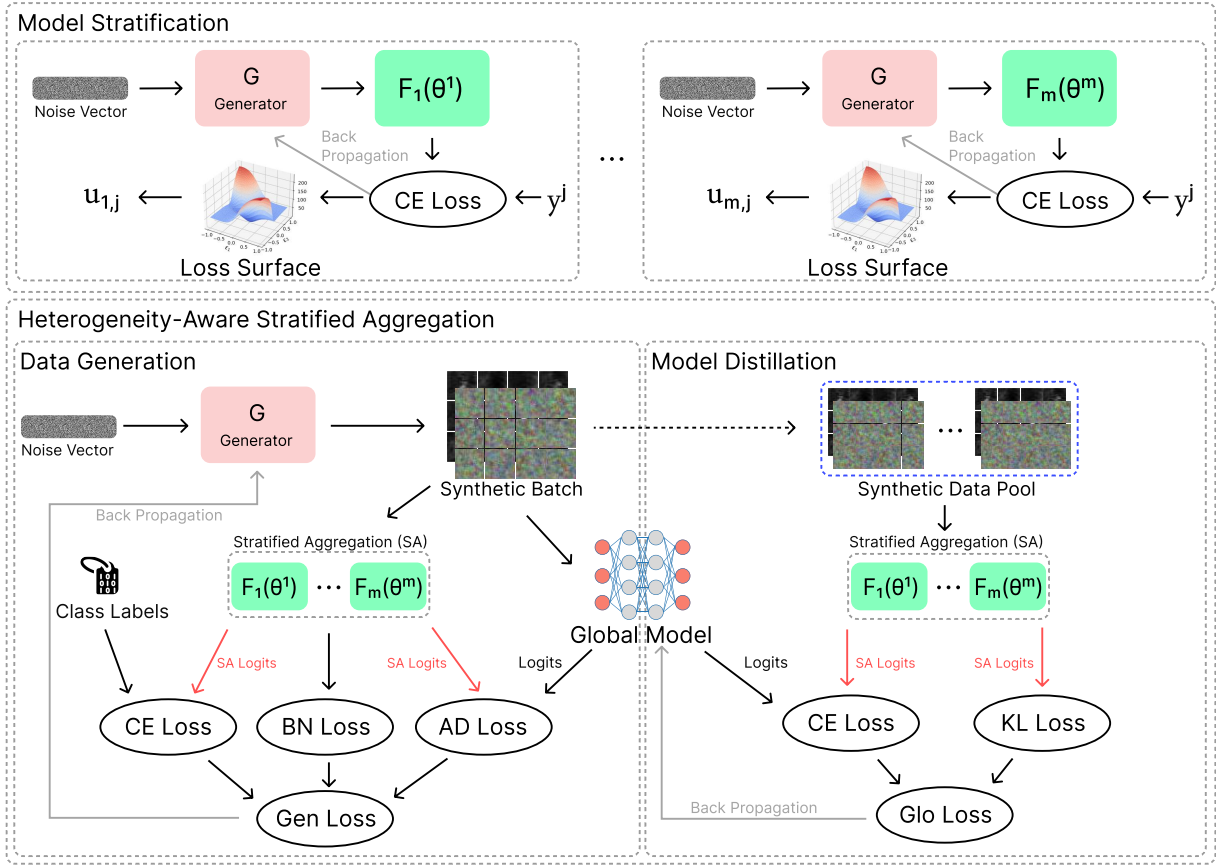


Figure 2: Illustration of the FedHydra framework. FedHydra consists of two stages: (1) the MS stage, which evaluates the classification capabilities of uploaded converged client models, and (2) the HASA stage, which enables data-free distillation training of the global model through two phases—data generation and model distillation.

iteration, we can calculate the following cross-entropy (CE) loss:

$$\ell_{k,j}^t(\hat{x}_t^j, y_t^j; \theta^k) = CE(F(\hat{x}_t^j; \theta^k), y_t^j), \quad (1)$$

where \hat{x}_t^j and y_t^j denotes the generated samples and assigned labels. After the entire T_G iterations, we can obtain the corresponding loss variance denoted as $L_{k,j} = [\ell_{k,j}^1, \dots, \ell_{k,j}^t, \dots, \ell_{k,j}^{T_G}]$. Since greater loss variance and a lower minimum loss value indicate stronger guidance from the teacher model to the Generator [2, 4, 11], the guidance capability of the client model $F_k(\theta^k)$ to the class j can be defined as

$$u_{k,j} = \frac{\max(L_{k,j}) - \min(L_{k,j})}{\min(L_{k,j})}. \quad (2)$$

Based on this, we can obtain a basic guidance capability matrix with a size of $c \times m$ for all client models across all class labels as

$$U = ([u_{k,j}]_{m \times c})^T. \quad (3)$$

Each row of U represents the guidance capability for a specific class label across all client models, while each column reflects the guidance capability of a single client model across all class labels. To realize the SA for prediction logits of client models, we need to compare the measure values in U to attain relative importance weights of guidance capability of a particular client model across

all class labels as well as for a particular class label across all client models. So we first normalize each row of U to $[0, 1]$ by

$$\bar{u}_{k,j} = \frac{u_{k,j}}{\sum_{k=1}^m u_{k,j}}. \quad (4)$$

The final normalized U by row can be defined as follows:

$$\bar{U}_r = ([\bar{u}_{k,j}]_{m \times c})^T, \quad (5)$$

wherein $\sum_{k=1}^m \bar{u}_{k,j} = 1$. Each row vector of \bar{U}_r represents the stratified weights for prediction logits from all client models for a particular class sample.

Then, we normalize each column of U to $[0, 1]$ as follows:

$$\hat{u}_{k,j} = \frac{u_{k,j}}{\sum_{j=1}^c u_{k,j}}. \quad (6)$$

The final normalized U by column is defined as

$$\bar{U}_c = ([\hat{u}_{k,j}]_{m \times c})^T, \quad (7)$$

wherein $\sum_{j=1}^c \hat{u}_{k,j} = 1$. Each column vector of \bar{U}_c represents the stratified weights for prediction logits of a particular client model across all class labels. The detailed procedure for conducting the MS is provided in **Algorithm 2**.

Algorithm 1 FedHydra Algorithm

```

1: Input: Client models  $\{F_k(\cdot)\}_{k=1}^m$  with parameters  $\{\theta^k\}_{k=1}^m$ , the
   global model  $F_g(\cdot)$  with parameter  $\theta^g$ , the Generator  $G(\cdot)$  with
   parameter  $\theta_G$ , class labels  $\{y^j\}_{j=1}^c$ , the global model training
   epochs  $T_g$  and learning rate  $\eta_g$ , and the generator training epochs
    $T_G$  and learning rate  $\eta_G$ .
2: Output: Well trained global model  $\theta^g$ 
3: procedure FedHydra():
4:   for each client model  $\theta^k$  in parallel do
5:      $\theta^k \leftarrow \text{LocalUpdate}(k)$ 
6:     Upload converged  $\theta^k$  to the server
7:   end for
8:   // model stratification
9:    $\bar{U}_r, \bar{U}_c \leftarrow \text{ModelStratification}(\{\theta^k\}_{k=1}^m, \theta_G, \{y^j\}_{j=1}^c)$ 
10:                                      $\triangleright$  See Algorithm 2.
11:   Initialize  $\theta^g$  and  $\theta_G$ 
12:   for each global training epoch  $t_g$  from 1 to  $T_g$  do
13:     Sample a batch of noises and labels  $\{z_i, y_i\}_{i=1}^b$ , denoted
14:     as  $\mathbf{z} = \{z_i\}_{i=1}^b$  and  $\mathbf{y} = \{y_i\}_{i=1}^b$ 
15:     // data generation
16:     for each generator training epoch  $t$  from 1 to  $T_G$  do
17:       Generate synthetic data  $\hat{\mathbf{x}} = \{\hat{x}_i\}_{i=1}^b \leftarrow G(\mathbf{z}; \theta_G^t)$ 
18:       Compute the loss  $\mathcal{L}_{Gen}$  by Eq. (16)
19:                                      $\triangleright$  See Algorithm 3 for SA computation.
20:        $\theta_G^{t+1} \leftarrow \theta_G^t - \eta_G \nabla_{\theta_G^t} \mathcal{L}_{Gen}$ 
21:     end for
22:     // model distillation
23:     Compute the loss  $\mathcal{L}_{Glo}$  by Eq. (19)
24:      $\theta_{t_g+1}^g \leftarrow \theta_{t_g}^g - \eta_g \nabla_{\theta_{t_g}^g} \mathcal{L}_{Glo}$ 
25:   end for
26:   return  $\theta^g$ 
27: end procedure

```

3.3 Heterogeneity-Aware Stratified Aggregation

HASA consists of two phases, Data Generation and Model Distillation, both incorporating **SA** to enhance the learning process.

3.3.1 Stratified Aggregation. For batch-generated samples by Generator and assigned target labels $(\mathbf{x}, \mathbf{y}) = \{x_i, y_i^j\}_{i=1}^b$ with size b , each client model on \mathbf{x} will output its batch prediction logits denoted as $P_k = F_k(\mathbf{x}; \theta^k)$ with size $b \times c$.

Based on Eq. (7), we first conduct an in-model weighted batch prediction logits \hat{P}_k for each P_k by

$$\hat{P}_k = P_k \odot (\mathbf{1}_{b \times 1} \times (\bar{U}_c(:, k))^T), \quad (8)$$

wherein \odot means the Hadamard product, $\mathbf{1}_{b \times 1}$ represents a column vector of size $b \times 1$ filled with ones, and $\bar{U}_c(:, k)$ denotes the k^{th} column of \bar{U}_c . Then, we can obtain in-model weighted prediction logits set P^i for the i^{th} in-batch sample across all client models as:

$$P^i = \begin{bmatrix} \hat{P}_1(i, :) \\ \vdots \\ \hat{P}_k(i, :) \\ \vdots \\ \hat{P}_m(i, :) \end{bmatrix}_{m \times c} \quad (i = 1, 2, \dots, b), \quad (9)$$

Algorithm 2 Model Stratification

```

1: Input: Client models  $\{F_k(\theta^k)\}_{k=1}^m$ , the Generator  $G(\theta_G)$  and
   class labels  $\{y^j\}_{j=1}^c$ 
2: Output: Stratified weight matrices  $\bar{U}_r$  and  $\bar{U}_c$ 
3: procedure ModelStratification( $\{\theta^k\}_{k=1}^m, \theta_G, \{y^j\}_{j=1}^c$ ):
4:   for each client model  $\theta^k, k$  from 1 to  $m$  do
5:     for each class label  $y^j, j$  from 1 to  $c$  do
6:       Initialize the Generator parameter  $\theta_G$ 
7:       Sample a batch of noise vectors and labels
8:        $\{z_i, y_i^j\}_{i=1}^b$ , denoted as  $\mathbf{z} = \{z_i\}_{i=1}^b$  and  $\mathbf{y} = \{y_i^j\}_{i=1}^b$ 
9:       // evaluate the guidance capability by Generator
10:      for each training epoch  $t$  from 1 to  $T_G$  do
11:         $\hat{\mathbf{x}} = \{\hat{x}_i\}_{i=1}^b \leftarrow G(\mathbf{z}; \theta_G^t)$ 
12:         $\ell_{k,j}^t \leftarrow CE(F_k(\hat{\mathbf{x}}; \theta^k), \mathbf{y})$ 
13:         $L_{k,j} \leftarrow \ell_{k,j}^t$ 
14:         $\theta_G^{t+1} \leftarrow \theta_G^t - \eta_G \nabla_{\theta_G^t} \ell_{k,j}^t$ 
15:      end for
16:      Compute  $u_{k,j}$  based on  $L_{k,j}$  using Eq. (2)
17:       $U \leftarrow u_{k,j}$ 
18:    end for
19:  end for
20:  Compute  $\bar{U}_r$  and  $\bar{U}_c$  from  $U$  using Eqs. (5) and (7)
21:  return  $\bar{U}_r$  and  $\bar{U}_c$ 
22: end procedure

```

wherein $\hat{P}_k(i, :)$ means the i^{th} row of \hat{P}_k . Subsequently, based on Eq. (5), the weight set for the guidance capability of all client models on batch samples can be calculated by

$$V = \begin{bmatrix} \bar{U}_r(\mathbf{y}(1), :) \\ \vdots \\ \bar{U}_r(\mathbf{y}(i), :) \\ \vdots \\ \bar{U}_r(\mathbf{y}(b), :) \end{bmatrix}_{b \times m}, \quad (10)$$

wherein $\mathbf{y}(i)$ denotes the i^{th} target class label and $\bar{U}_r(\mathbf{y}(i), :)$ means the $\mathbf{y}(i)^{\text{th}}$ row of \bar{U}_r . Combining Eq. (9) and Eq. (10), the inter-model weighted batch prediction logits P can be calculated by

$$P = \begin{bmatrix} V(1, :) \times P^1 \\ \vdots \\ V(i, :) \times P^i \\ \vdots \\ V(b, :) \times P^b \end{bmatrix}_{b \times c}, \quad (11)$$

wherein $V(i, :)$ represents the i^{th} row of V , and P is the final ensemble prediction logits output, termed **Stratified Aggregation (SA)**. The specific computation process is summarized in Algorithm 3.

3.3.2 Data Generation. In this phase, our goal is to train a generator guided by client models to produce synthetic data that closely aligns with the distribution of the aggregated client data. Inspired by [39], we approach generator training from three key aspects.

We first compute the **SA** prediction logits with Algorithm 3 for a batch-generated data $\hat{\mathbf{x}} = G(\mathbf{z}; \theta_G)$ and their assigned labels \mathbf{y} , as:

$$P = \text{SA}(\hat{\mathbf{x}}, \mathbf{y}, \{\theta^k\}_{k=1}^m), \quad (12)$$

Algorithm 3 *Stratified Aggregation (SA)*

-
- 1: **Input:** Client models $\{F_k(\theta^k)\}_{k=1}^m$, two weight matrices \bar{U}_r and \bar{U}_c from model stratification, and synthetic batch data $(\hat{\mathbf{x}}, \mathbf{y}) = \{x_i, y_i\}_{i=1}^b$
 - 2: **Output:** weighted batch prediction logits matrix P
 - 3: **procedure SA** ($\{\theta^k\}_{k=1}^m, \bar{U}_r, \bar{U}_c, (\hat{\mathbf{x}}, \mathbf{y})$)
 - 4: **for** each client model θ^k , k from 1 to m **do**
 - 5: $P_k \leftarrow F_k(\mathbf{x}; \theta^k)$
 - 6: Compute in-model weighted prediction logits \hat{P}_k based on P_k and \bar{U}_c using Eq. (8)
 - 7: **end for**
 - 8: Compute inter-model weighted prediction logits P based on $\{\hat{P}_k\}_{k=1}^m$ and \bar{U}_r using Eqs. (9), (10), and (11)
 - 9: return P
 - 10: **end procedure**
-

where P is our proposed **SA** logits. Then, to ensure the distribution similarity between synthetic data and real client data, we minimize the cross-entropy (CE) loss between P and \mathbf{y} , defined in Eq. (13), in the training objective function of the generator.

$$\mathcal{L}_{CE}(\hat{\mathbf{x}}, \mathbf{y}; \theta_G) = CE(P, \mathbf{y}). \quad (13)$$

Second, Batch Normalization (BN) loss introduced in [39] is also employed to increase the stability of generator training, defined as:

$$\mathcal{L}_{BN}(\hat{\mathbf{x}}; \theta_G) = \frac{1}{m} \sum_{k=1}^m \sum_l \left(\|\mu_l(\hat{\mathbf{x}}) - \mu_{k,l}(\hat{\mathbf{x}})\| + \|\sigma_l^2(\hat{\mathbf{x}}) - \sigma_{k,l}^2(\hat{\mathbf{x}})\| \right), \quad (14)$$

where $\mu_l(\hat{\mathbf{x}})$ and $\sigma_l^2(\hat{\mathbf{x}})$ are the batch-wise mean and variance of hidden features from the l^{th} BN layer of the generator, $\mu_{k,l}(\hat{\mathbf{x}})$ and $\sigma_{k,l}^2(\hat{\mathbf{x}})$ are the mean and variance of the l^{th} BN layer of the k^{th} client model.

Third, to increase the diversity of generated data, an adversarial distillation (AD) loss is considered to maximize the discrepancy between **SA** logits and prediction logits of the global model as:

$$\mathcal{L}_{AD}(\hat{\mathbf{x}}, \mathbf{y}; \theta_G) = -KL(P, F_g(\hat{\mathbf{x}}; \theta^g)), \quad (15)$$

where $F_g(\cdot)$ and θ^g denote the global model and its parameter. Therefore, the final generator training loss is defined by combining the above three loss terms, as follows:

$$\mathcal{L}_{Gen}(\hat{\mathbf{x}}, \mathbf{y}; \theta_G) = \mathcal{L}_{CE}(\hat{\mathbf{x}}, \mathbf{y}; \theta_G) + \lambda_1 \mathcal{L}_{BN}(\hat{\mathbf{x}}; \theta_G) + \lambda_2 \mathcal{L}_{AD}(\hat{\mathbf{x}}, \mathbf{y}; \theta_G), \quad (16)$$

where λ_1 and λ_2 are adjustable parameters.

3.3.3 Model Distillation. Based on the synthetic data produced in the data generation phase, we design a new model distillation scheme to train our global model with knowledge distillation techniques.

We consider the two loss terms in the training objective function of the global model. First, we use the KL loss between the **SA** logits and prediction logits of the global model to distill the knowledge from client models to the global model, defined as:

$$\mathcal{L}_{KL}(\hat{\mathbf{x}}, \mathbf{y}; \theta^g) = KL(P, F_g(\hat{\mathbf{x}}; \theta^g)). \quad (17)$$

To achieve efficient and stable model distillation, ensuring consistent prediction labels between the ensemble client models and the

global model is crucial, especially considering the potential deviation between synthetic and real data. So, we introduce the following CE loss, defined as:

$$\mathcal{L}_{\widehat{CE}}(\hat{\mathbf{x}}, \mathbf{y}; \theta^g) = CE(F_g(\hat{\mathbf{x}}; \theta^g), H[P]), \quad (18)$$

where $H[\cdot]$ represents to obtain the hard label of prediction logits. Therefore, by combining the above two loss terms, the final training loss function for realizing model distillation is defined as follows:

$$\mathcal{L}_{Glo}(\hat{\mathbf{x}}, \mathbf{y}; \theta^g) = \mathcal{L}_{KL}(\hat{\mathbf{x}}, \mathbf{y}; \theta^g) + \beta \mathcal{L}_{\widehat{CE}}(\hat{\mathbf{x}}, \mathbf{y}; \theta^g), \quad (19)$$

where β is an adjustable parameter.

4 Experiments

4.1 Setup

4.1.1 Datasets. Our evaluation experiments utilize four widely used datasets: MNIST [16], FashionMNIST [36], SVHN [25], and CIFAR-10 [15]. MNIST consists of 60,000 training and 10,000 testing grayscale images of handwritten digits, each of size 28×28 . FashionMNIST shares the same data structure with MNIST but contains images of fashion items. SVHN comprises over 600,000 color images of house numbers from Google Street View, making it suitable for real-world digit recognition. CIFAR-10 consists of 60,000 color images of size 32×32 across 10 object categories, with a 50,000/10,000 train-test split. These datasets provide diverse benchmarks for evaluating FL performance.

4.1.2 Client Data Distribution. We adopt the Dirichlet distribution method ($Dir(\alpha)$) in [38] to simulate diverse client data distributions in practical FL scenarios. Adjusting the parameter α allows us to modify the level of data heterogeneity: a lower α results in more pronounced heterogeneity in the data distribution, while a higher α results in a homogeneous data distribution. We consider four cases, $\alpha = \{0.5, 0.3, 0.1, 0.01\}$, ranging from a more homogeneous distribution ($\alpha = 0.5$) to a highly heterogeneous distribution ($\alpha = 0.01$). Unless otherwise specified, we use $\alpha = 0.5$ as the default setting.

4.1.3 Models. The generator introduced in FedHydra begins with a fully connected layer that transforms the input noise vector into a 2D feature map. This is followed by three upsampling convolutional layers, each consisting of batch normalization, LeakyReLU activation, and 2D transposed convolutions. The final layer uses a Sigmoid activation function to output either a 32×32 RGB image or a 28×28 grayscale image. For client models, we employ a two-layer CNN for MNIST and FashionMNIST, and a three-layer CNN for SVHN and CIFAR-10 in the case of homogeneous model architecture. In model heterogeneity scenarios, more complex architectures, such as GoogleNet, ResNet18, and LeNet, are utilized in our experiments. The detailed model architectures are described in the appendix G.

4.1.4 Baselines. Since the proposed method aims to address the heterogeneity problem in OSFL, we omit the comparison with conventional FL baselines, such as FedProx [19], FedNova [34], SCAFFOLD [14], and FedGen [43], which are specifically designed for multi-round federated optimization rather than single-round FL. Furthermore, we do not compare our method with FEDCVAE [10], as it directly embeds the data on the client side and uploads it to the server without client-side model training. Instead, we evaluate the

performance of FedHydra against five SOTA baselines: FedAvg [22], OT [31], FedDF [20], DENSE [39], and Co-Boosting [5].

4.1.5 Hyperparameter Configurations. In our OSFL setup, we consider various numbers of clients $m = \{5, 10, 20, 50, 100\}$, with the default setting of $m = 5$. For the client model training, we employ the SGD optimizer with learning rate $\eta = 0.01$, while setting the local epochs and batch size as $B = 128$ and $E = 200$, respectively. On the server side, we utilize the Adam optimizer with learning rate $\eta_G = 0.001$ to train the generator. This generator, characterized by adjustable parameters $\lambda_1 = 1.0, \lambda_2 = 1.0$, undergoes training for $T_G = 30$ rounds to generate batch examples. For the distillation training of the global model, we set the training epochs to $T_g = 200$ and the learning rate to $\eta_g = 0.01$, with SGD serving as the optimizer.

4.2 Evaluation

4.2.1 Performance Overview. FedHydra demonstrates superior performance across various data heterogeneity settings compared to existing methods, including FedAvg, OT, FedDF, DENSE, and Co-Boosting. As shown in Table 1, FedHydra consistently achieves the highest accuracy across all datasets and values of α , indicating strong robustness against heterogeneous data distribution.

For MNIST, most methods perform well under low heterogeneity ($\alpha = 0.5$) but degrade as it increases. FedAvg drops sharply from 81.89% to 10.10%, with FedDF and DENSE showing similar trends. Co-Boosting improves stability but is outperformed by FedHydra, which achieves 38.83% at $\alpha = 0.01$, surpassing Co-Boosting by 9.72%. On FashionMNIST and SVHN, FedHydra maintains the highest accuracy, outperforming the second-best method by up to 9.01% at $\alpha = 0.01$. For CIFAR10, FedHydra reaches 40.63%, exceeding Co-Boosting by 5.53% and significantly outperforming FedAvg and OT under extreme data heterogeneity.

FedHydra’s robustness comes from its superior handling of severe data heterogeneity. While FedAvg struggles with parameter averaging and FedDF/DENSE fails under extreme settings, Co-Boosting improves but remains inferior. These results confirm FedHydra as the most effective OSFL method in heterogeneous environments. Further experiments analyze accuracy trends over distillation epochs across four datasets. Fig. 3 shows that FedHydra surpasses SOTA methods after 50 epochs, especially when $\alpha \leq 0.3$. However, all the models collapse due to overfitting in model distillation, likely caused by small data sizes or single-class clients. In Fig. 4, FedHydra dominates on CIFAR10, consistently outperforming baselines from 25 to 200 epochs under $\alpha = \{0.5, 0.3, 0.1, 0.01\}$.

4.2.2 Impact of Stratified Aggregation. To validate the effectiveness of SA under heterogeneous federated distributions, we introduce an extreme $2c/c$ scenario where each client possesses only two disjoint class samples. Fig. 5 (a) illustrates this distribution for MNIST across five clients. As shown in Fig. 5 (b), each client model excels primarily in its two assigned classes, with classification weights near 1 (e.g., client 1 has 0.9594 for class 0 and 0.9797 for class 1, while other weights are close to zero). This confirms that our MS accurately captures client classification capabilities.

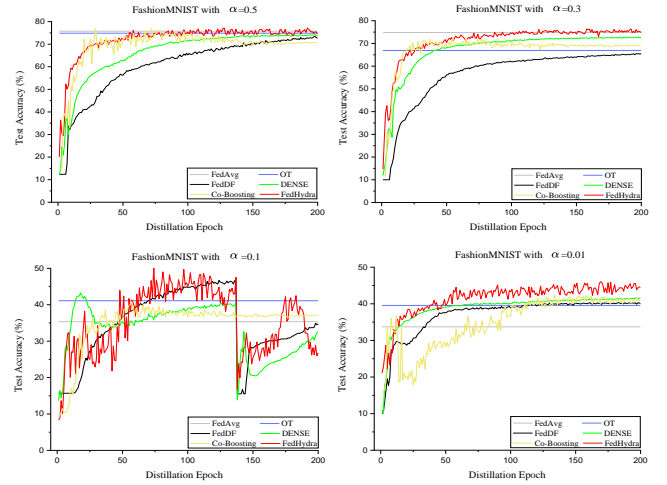


Figure 3: Test accuracy versus distillation epoch over FashionMNIST with $\alpha = \{0.5, 0.3, 0.1, 0.01\}$.

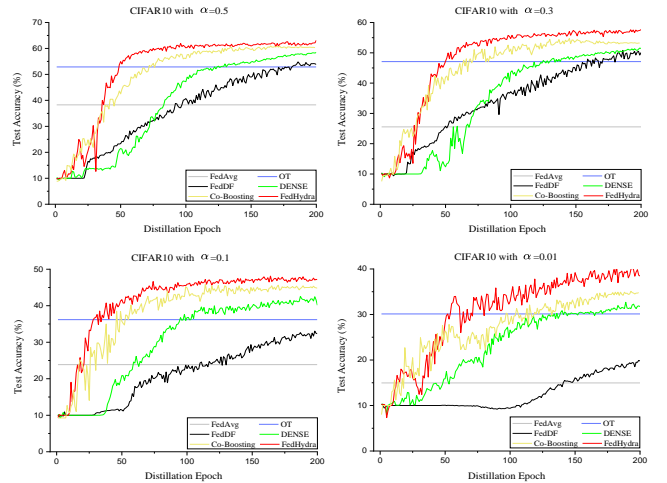


Figure 4: Test accuracy versus distillation epoch over CIFAR10 with $\alpha = \{0.5, 0.3, 0.1, 0.01\}$.

To evaluate the performance under $2c/c$ distribution, Table 2 presents the top-1 test accuracy on four datasets. FedHydra consistently outperforms all baseline methods, achieving the highest accuracy. Among the baselines, OT performs the worst across all datasets. Co-Boosting shows competitive results, especially on SVHN and CIFAR10, but still lags behind FedHydra. FedDF and DENSE perform worse than FedAvg on simpler datasets (MNIST, FashionMNIST), while FedAvg struggles on complex datasets (SVHN, CIFAR10). These results confirm the robustness of FedHydra under $2c/c$ distribution. Test accuracy trends are shown in Fig. 6, further demonstrating FedHydra’s superiority.

Furthermore, we compare the test accuracy of the averaging ensemble (AE) from DENSE and our SA across four datasets, as shown in Fig. 7. The results show that SA consistently outperforms AE, with up to a 20.00% gap at $\alpha = 0.5$ and 0.3. As data heterogeneity increases, AE performance drops sharply, e.g., from 81.75% to 37.41%

Table 1: Top-1 test accuracy achieved by baselines and our FedHydra over various datasets with varying α .

Dataset	MNIST				FashionMNIST				SVHN				CIFAR10			
	$\alpha=0.5$	$\alpha=0.3$	$\alpha=0.1$	$\alpha=0.01$												
FedAvg	81.89	69.89	25.96	10.10	75.76	74.81	35.35	33.71	65.50	64.64	31.46	21.94	38.26	25.54	23.87	14.96
OT	77.45	77.32	50.18	25.63	74.88	66.91	41.10	39.56	78.24	69.58	55.02	15.36	52.88	47.10	36.19	30.12
FedDF	78.23	73.59	31.52	10.10	73.44	65.61	46.68	40.36	80.20	81.00	54.35	7.59	54.81	50.82	33.06	19.91
DENSE	77.86	76.78	36.73	11.17	74.20	72.79	43.26	41.65	79.44	78.81	53.69	7.75	58.48	51.57	42.56	32.69
Co-Boosting	86.76	83.47	44.76	29.11	75.89	72.91	47.20	42.38	81.06	76.64	57.59	14.45	62.88	54.74	45.83	35.10
FedHydra (ours)	88.75	85.16	59.97	38.83	77.20	76.39	50.48	46.02	82.39	82.96	62.08	30.95	63.15	57.66	48.12	40.63

Table 2: Top-1 test accuracy achieved by baselines and FedHydra over various datasets with 2c/c distribution.

Dataset	MNIST	FashionMNIST	SVHN	CIFAR10
FedAvg	20.50	32.73	26.68	9.22
OT	8.92	16.98	17.63	12.15
FedDF	13.38	15.33	42.03	24.28
DENSE	15.58	22.31	41.38	31.36
Co-Boosting	26.05	18.22	42.38	33.84
FedHydra (ours)	40.81	39.06	50.61	39.09

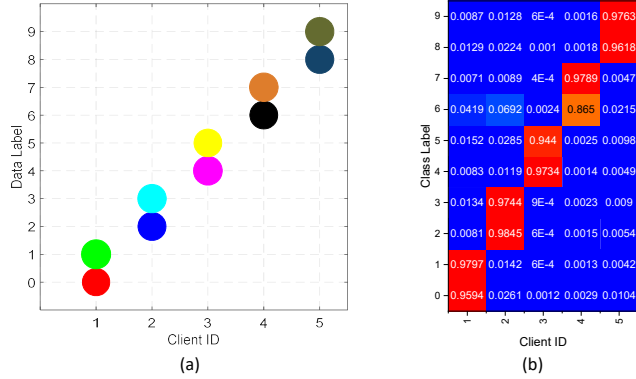


Figure 5: Visualization of SA. (a) 2c/c data distribution across five clients using MNIST as an example. (b) The weight distribution of evaluated classification capability for five client models on ten class labels.

on MNIST when $\alpha = 0.1$. The gap is largest at $\alpha = 0.01$, which represents both label and size heterogeneity, whereas 2c/c maintains equal sizes.

4.2.3 Impact of Stratified Aggregation Guided Model Distillation. We evaluate the impact of our SA-guided model distillation by comparing it with the five SOTA methods, and FedHydra on CIFAR10 with $\alpha = 0.1$. The results are illustrated in Fig. 8. Fig. 8 (a) shows test accuracy across local training epochs $E = \{40, 80, 120, \dots, 400\}$. The FedAvg achieves its best accuracy ($\sim 24.00\%$) at $E = 40$, but performance deteriorates with increasing E due to weight divergence under data heterogeneity. Fig. 8 (b) compares different methods over $E \in [0, 400]$. FedHydra consistently outperforms SOTA methods, and client models, while FedAvg performs worse than individual clients. OT and Co-Boosting improve over FedAvg but remain below FedHydra. These results confirm the robustness of SA-guided model distillation, demonstrating its superior handling of heterogeneous data distributions.

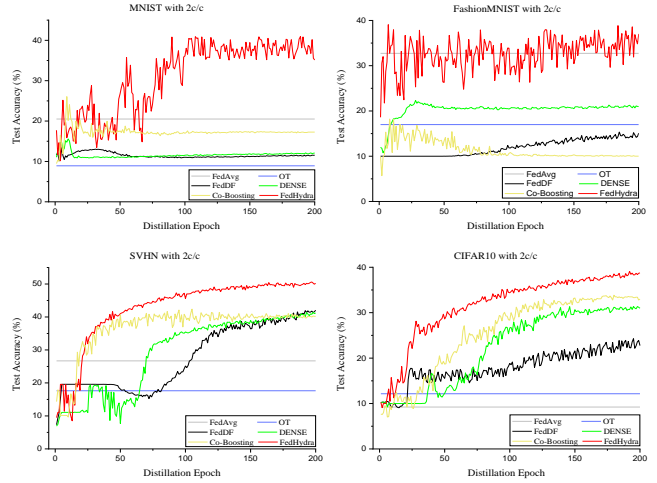


Figure 6: Test accuracy versus distillation epoch over diverse datasets with 2c/c distribution.

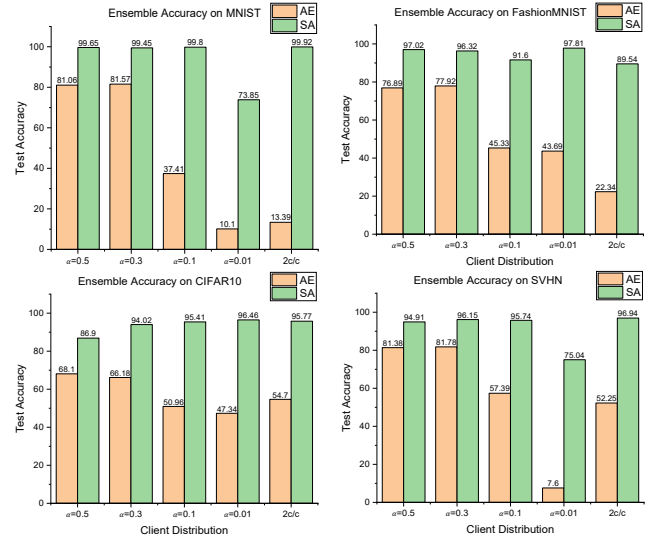


Figure 7: Test accuracy achieved by AE and our SA over four datasets with varying client data distributions.

4.2.4 Performance Comparison under OSFL Model Heterogeneity. FedHydra effectively addresses data and model heterogeneity. We evaluate its performance on CIFAR10 using five client models (GoogleNet, ResNet18, two CNNs, and LeNet) across varying α values. Since FedAvg and OT do not support model heterogeneity,

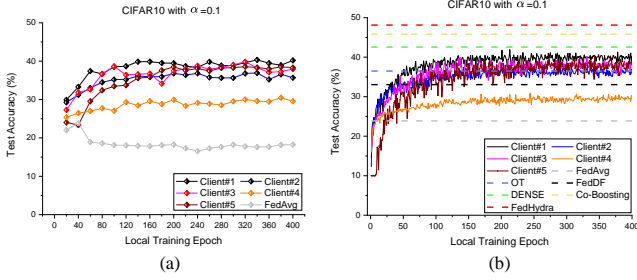


Figure 8: (a) Test accuracy of FedAvg and client models across local training epochs $E = 20, 40, 60, \dots, 400$. (b) Local training accuracy of different clients. The dotted lines represent the top-1 test accuracy achieved by baselines and our FedHydra.

Table 3: Top-1 test accuracy achieved by baselines and FedHydra over CIFAR10 with personalized client models. M1 to M5 correspond to GoogleNet, ResNet18, two customized CNN models, and LeNet, respectively.

α	Personalized Client Model					Server (ResNet18)			
	M1	M2	M3	M4	M5	FedDF	DENSE	Co-Boosting	FedHydra
$\alpha=0.01$	26.68	28.78	26.71	19.28	10.00	22.25	18.67	25.63	30.51
$\alpha=0.1$	37.36	36.63	35.60	30.41	28.77	27.39	26.43	26.82	30.90
$\alpha=0.3$	46.41	55.49	45.78	47.98	33.47	46.96	44.54	45.61	48.80
$\alpha=0.5$	49.33	61.08	47.65	54.14	48.25	56.27	51.29	53.76	59.23

we compare FedHydra with FedDF, DENSE, and Co-Boosting. As shown in Table 3, FedHydra consistently outperforms all baselines, achieving 59.23% at $\alpha = 0.5$. As α decreases, FedDF and DENSE drop sharply to 22.25% and 18.67% at $\alpha = 0.01$, while FedHydra maintains robustness with 30.51%, demonstrating superior adaptability. Additional results on SVHN are in Appendix D.

Table 4: Top-1 test accuracy achieved by baselines and FedHydra over SVHN with different client numbers $K = \{5, 10, 20, 50, 100\}$.

Client K	FedAvg	OT	FedDF	DENSE	Co-Boosting	FedHydra
5	65.50	78.24	80.20	79.44	81.06	82.39
10	43.45	58.62	70.20	69.51	75.92	77.13
20	47.87	56.76	69.36	69.10	70.01	76.54
50	36.77	45.68	68.30	67.74	67.93	74.89
100	23.69	35.23	50.37	48.87	53.64	60.01

4.2.5 Impact of Client Numbers. The number of clients (K) significantly impacts OSFL performance, as increasing K intensifies data fragmentation and heterogeneity. Table 4 shows that as K grows, accuracy declines across all methods. FedHydra consistently achieves the highest accuracy. FedDF and DENSE remain stable but drop significantly at $K = 100$, while Co-Boosting struggles with larger K . FedAvg and OT perform the worst, with FedAvg falling from 65.50% at $K = 5$ to 23.69% at $K = 100$. These results highlight FedHydra’s robustness in large-client federated settings. More CIFAR10 experiments are in Appendix C.1.

4.2.6 Performance Under Multiple Global Training Rounds. Global training rounds (T) are crucial in FL, affecting convergence and final performance. Table 5 shows CIFAR10 accuracy at $\alpha =$

Table 5: Top-1 test accuracy achieved by baselines and FedHydra over CIFAR10 with $\alpha = 0.1$ under multiple global rounds.

Global round	FedAvg	OT	FedDF	DENSE	Co-Boosting	FedHydra
$T=1$	22.72	18.33	21.33	29.60	31.68	37.95
$T=2$	37.32	26.38	28.63	32.39	37.93	46.52
$T=3$	35.95	39.54	30.36	36.42	46.23	48.75
$T=4$	43.86	36.88	30.71	38.85	46.84	50.17
$T=5$	41.99	39.96	28.82	37.27	45.20	49.34

0.1 across different T values. FedHydra consistently outperforms all methods, reaching 50.17% at $T = 4$. FedAvg, OT, and FedDF fluctuate, while Co-Boosting and DENSE improve but stay below FedHydra. FedAvg peaks at $T = 4$ but declines at $T = 5$, indicating instability. These results confirm FedHydra’s robustness in multi-round FL. More SVHN experiments are in Appendix C.2 and E.

4.2.7 Time Complexity Analysis. We briefly compare the time complexity of our FedHydra algorithm with DENSE, the primary baseline. Assume that the time complexity (TC) of completing one batch training round of generator is $O(1)$. Without considering the TC of the global model training, the total TC for DENSE is $O(T_g \cdot T_G)$ while for our FedHydra it is $O((m \cdot c + T_g) \cdot T_G)$. Considering the computation capability of the central server and limited client numbers m and classes c , we believe the increased TC of $O(m \cdot c \cdot T_G)$ is acceptable in practical FL applications when comparing between FedHydra and DENSE. The results of five repeated experiments with running time (seconds) on CIFAR10 are shown in Appendix F, where we compare the computational complexity of FedHydra and DENSE. Our results show that FedHydra performs better in heterogeneous scenarios, with only a 7% increase in computational complexity compared to DENSE, which we consider acceptable.

Table 6: Top-1 test accuracy achieved by FedHydra over various datasets with varying λ_1 and λ_2 .

λ_1	λ_2	MNIST	FashionMNIST	SVHN	CIFAR10
1.0	1.0	88.75	77.20	82.39	63.15
0.5	1.0	84.61	76.72	81.80	62.11
0.0	1.0	83.29	76.07	80.96	60.18
1.0	0.5	81.54	73.72	78.04	56.92
1.0	0.0	76.19	70.64	76.12	52.15
0.0	0.0	74.14	69.38	75.93	50.65

4.2.8 Ablation Study. λ in Eq. (16) serves as a loss adjustment factor, where λ_1 regulates the BN loss and λ_2 controls the AD loss. To evaluate their impact, we conducted experiments with varying λ_1 and λ_2 , with results summarized in Table 6. The findings indicate that when $\lambda_1 = \lambda_2 = 0$, both BN and AD losses are inactive, leading to a significant decline in FedHydra’s performance. Notably, variations in AD loss (λ_2) have a more pronounced effect compared to BN loss (λ_1). Overall, both losses contribute significantly to enhancing the generator’s performance within the FedHydra framework.

5 Conclusion

In this work, we present FedHydra, a data-free OSFL framework designed to tackle both data and model heterogeneity. Unlike existing OSFL approaches that address only one aspect of heterogeneity, FedHydra employs a two-stage learning strategy: **MS** to evaluate client models' classification strengths and **HASA** to refine aggregation via a data-free distillation framework. Experimental results across multiple benchmarks demonstrate that FedHydra consistently surpasses SOTA OSFL methods in both homogeneous and heterogeneous environments. FedHydra provides a practical and scalable solution for OSFL. Future research will focus on extending its adaptability to more complex heterogeneity scenarios and optimizing computational efficiency.

References

- [1] Durmus Alp Emre Acar, Yue Zhao, Ramon Matas, Matthew Mattina, Paul Whatmough, and Venkatesh Saligrama. 2020. Federated Learning Based on Dynamic Regularization. In *International Conference on Learning Representations*.
- [2] Xiaoyu Cao, Jinyuan Jia, and Neil Zhenqiang Gong. 2021. Provably secure federated learning against malicious clients. In *Proceedings of the AAAI conference on artificial intelligence*, Vol. 35. 6885–6893.
- [3] Hanting Chen, Yunhe Wang, Chang Xu, Zhaohui Yang, Chuanjian Liu, Boxin Shi, Chunjing Xu, Chao Xu, and Qi Tian. 2019. Data-free learning of student networks. In *Proceedings of the IEEE/CVF international conference on computer vision*. 3514–3522.
- [4] Xinlei Chen and Kaiming He. 2021. Exploring simple siamese representation learning. In *Proceedings of the IEEE/CVF conference on computer vision and pattern recognition*. 15750–15758.
- [5] Rong Dai, Yonggang Zhang, Ang Li, Tongliang Liu, Xun Yang, and Bo Han. 2024. Enhancing One-Shot Federated Learning Through Data and Ensemble Co-Boosting. (2024).
- [6] Don Kurian Dennis, Tian Li, and Virginia Smith. 2021. Heterogeneity for the win: One-shot federated clustering. In *International Conference on Machine Learning*. PMLR, 2611–2620.
- [7] Neel Guha, Ameet Talwalkar, and Virginia Smith. 2019. One-shot federated learning. *arXiv preprint arXiv:1902.11175* (2019).
- [8] Haibo He and Edward A Garcia. 2009. Learning from imbalanced data. *IEEE Transactions on knowledge and data engineering* 21, 9 (2009), 1263–1284.
- [9] Jingrui He. 2017. Learning from Data Heterogeneity: Algorithms and Applications.. In *IJCAI*. 5126–5130.
- [10] Clare Elizabeth Heinbaugh, Emilio Luz-Ricca, and Huajie Shao. 2022. Data-free one-shot federated learning under very high statistical heterogeneity. In *The Eleventh International Conference on Learning Representations*.
- [11] Fei Hu, Wuneng Zhou, Kaili Liao, Hongliang Li, and Dongbing Tong. 2023. Toward federated learning models resistant to adversarial attacks. *IEEE Internet of Things Journal* 10, 19 (2023), 16917–16930.
- [12] Wenke Huang, Mang Ye, and Bo Du. 2022. Learn from others and be yourself in heterogeneous federated learning. In *Proceedings of the IEEE/CVF Conference on Computer Vision and Pattern Recognition*. 10143–10153.
- [13] Malhar S Jere, Tyler Farnan, and Farinaz Koushanfar. 2020. A taxonomy of attacks on federated learning. *IEEE Security & Privacy* 19, 2 (2020), 20–28.
- [14] Sai Praneeth Karimireddy, Satyen Kale, Mehryar Mohri, Sashank Reddi, Sebastian Stich, and Ananda Theertha Suresh. 2020. Scaffold: Stochastic controlled averaging for federated learning. In *International conference on machine learning*. PMLR, 5132–5143.
- [15] Alex Krizhevsky, Geoffrey Hinton, et al. 2009. Learning multiple layers of features from tiny images. (2009).
- [16] Yann LeCun, Léon Bottou, Yoshua Bengio, and Patrick Haffner. 1998. Gradient-based learning applied to document recognition. *Proc. IEEE* 86, 11 (1998), 2278–2324.
- [17] Qinbin Li, Bingsheng He, and Dawn Song. 2021. Model-contrastive federated learning. In *Proceedings of the IEEE/CVF conference on computer vision and pattern recognition*. 10713–10722.
- [18] Qinbin Li, Bingsheng He, and Dawn Song. 2021. Practical One-Shot Federated Learning for Cross-Silo Setting. In *Proceedings of the Thirtieth International Joint Conference on Artificial Intelligence, IJCAI-21*. International Joint Conferences on Artificial Intelligence Organization, 1484–1490.
- [19] Tian Li, Anit Kumar Sahu, Manzil Zaheer, Maziar Sanjabi, Ameet Talwalkar, and Virginia Smith. 2020. Federated optimization in heterogeneous networks. *Proceedings of Machine learning and systems* 2 (2020), 429–450.
- [20] Tao Lin, Lingjing Kong, Sebastian U Stich, and Martin Jaggi. 2020. Ensemble distillation for robust model fusion in federated learning. *Advances in Neural Information Processing Systems* 33 (2020), 2351–2363.
- [21] Yuang Liu, Wei Zhang, Jun Wang, and Jianyong Wang. 2021. Data-free knowledge transfer: A survey. *arXiv preprint arXiv:2112.15278* (2021).
- [22] Brendan McMahan, Eider Moore, Daniel Ramage, Seth Hampson, and Blaise Aguera y Arcas. 2017. Communication-efficient learning of deep networks from decentralized data. In *Artificial intelligence and statistics*. PMLR, 1273–1282.
- [23] Matias Mendieta, Taojiannan Yang, Pu Wang, Minwoo Lee, Zhengming Ding, and Chen Chen. 2022. Local learning matters: Rethinking data heterogeneity in federated learning. In *Proceedings of the IEEE/CVF Conference on Computer Vision and Pattern Recognition*. 8397–8406.
- [24] Paul Micaelli and Amos J Storkey. 2019. Zero-shot knowledge transfer via adversarial belief matching. *Advances in Neural Information Processing Systems* 32 (2019).
- [25] Yuval Netzer, Tao Wang, Adam Coates, Alessandro Bissacco, Baolin Wu, Andrew Y Ng, et al. 2011. Reading digits in natural images with unsupervised feature learning. In *NIPS workshop on deep learning and unsupervised feature learning*, Vol. 2011. Granada, Spain, 7.
- [26] Liangqiong Qu, Yuyin Zhou, Paul Pu Liang, Yingda Xia, Feifei Wang, Ehsan Adeli, Li Fei-Fei, and Daniel Rubin. 2022. Rethinking architecture design for tackling data heterogeneity in federated learning. In *Proceedings of the IEEE/CVF conference on computer vision and pattern recognition*. 10061–10071.
- [27] Piyush Raikwar and Deepak Mishra. 2022. Discovering and overcoming limitations of noise-engineered data-free knowledge distillation. *Advances in Neural Information Processing Systems* 35 (2022), 4902–4912.
- [28] Bosen Rao, Jiale Zhang, Di Wu, Chengcheng Zhu, Xiaobing Sun, and Bing Chen. 2024. Privacy Inference Attack and Defense in Centralized and Federated Learning: A Comprehensive Survey. *IEEE Transactions on Artificial Intelligence* (2024), 1–22. <https://doi.org/10.1109/TAI.2024.3363670>
- [29] Felix Sattler, Tim Korjakow, Roman Rischke, and Wojciech Samek. 2021. Fedaux: Leveraging unlabeled auxiliary data in federated learning. *IEEE Transactions on Neural Networks and Learning Systems* 34, 9 (2021), 5531–5543.
- [30] MyungJae Shin, Chihoon Hwang, Joongheon Kim, Jihong Park, Mehdi Bennis, and Seong-Lyun Kim. 2020. Xor mixup: Privacy-preserving data augmentation for one-shot federated learning. *arXiv preprint arXiv:2006.05148* (2020).
- [31] Sidak Pal Singh and Martin Jaggi. 2020. Model fusion via optimal transport. *Advances in Neural Information Processing Systems* 33 (2020), 22045–22055.
- [32] Minxue Tang, Xuefei Ning, Yitu Wang, Jingwei Sun, Yu Wang, Hai Li, and Yiran Chen. 2022. FedCor: Correlation-based active client selection strategy for heterogeneous federated learning. In *Proceedings of the IEEE/CVF Conference on Computer Vision and Pattern Recognition*. 10102–10111.
- [33] Zhenheng Tang, Yonggang Zhang, Shaohuai Shi, Xin He, Bo Han, and Xiaowen Chu. 2022. Virtual homogeneity learning: Defending against data heterogeneity in federated learning. In *International Conference on Machine Learning*. PMLR, 21111–21132.
- [34] Jianyu Wang, Qinghua Liu, Hao Liang, Gauri Joshi, and H Vincent Poor. 2020. Tackling the objective inconsistency problem in heterogeneous federated optimization. *Advances in neural information processing systems* 33 (2020), 7611–7623.
- [35] Di Wu, Jun Bai, Yiliao Song, Junjun Chen, Wei Zhou, Yong Xiang, and Atul Sajjanhar. 2023. FedInverse: Evaluating Privacy Leakage in Federated Learning. In *The Twelfth International Conference on Learning Representations*.
- [36] Han Xiao, Kashif Rasul, and Roland Vollgraf. 2017. Fashion-mnist: a novel image dataset for benchmarking machine learning algorithms. *arXiv preprint arXiv:1708.07747* (2017).
- [37] Hongxu Yin, Pavlo Molchanov, Jose M Alvarez, Zhizhong Li, Arun Mallya, Derek Hoiem, Niraj K Jha, and Jan Kautz. 2020. Dreaming to distill: Data-free knowledge transfer via deepinversion. In *Proceedings of the IEEE/CVF Conference on Computer Vision and Pattern Recognition*. 8715–8724.
- [38] Mikhail Yurochkin, Mayank Agarwal, Soumya Ghosh, Kristjan Greenewald, Nghia Hoang, and Yasaman Khazaeni. 2019. Bayesian nonparametric federated learning of neural networks. In *International conference on machine learning*. PMLR, 7252–7261.
- [39] Jie Zhang, Chen Chen, Bo Li, Lingjuan Lyu, Shuang Wu, Shouhong Ding, Chunhua Shen, and Chao Wu. 2022. Dense: Data-free one-shot federated learning. *Advances in Neural Information Processing Systems* 35 (2022), 21414–21428.
- [40] Jiale Zhang, Junjun Chen, Di Wu, Bing Chen, and Shui Yu. 2019. Poisoning attack in federated learning using generative adversarial nets. In *2019 18th IEEE international conference on trust, security and privacy in computing and communications/13th IEEE international conference on big data science and engineering (TrustCom/BigDataSE)*. IEEE, 374–380.
- [41] Lin Zhang, Li Shen, Liang Ding, Dacheng Tao, and Ling-Yu Duan. 2022. Fine-tuning global model via data-free knowledge distillation for non-iid federated learning. In *Proceedings of the IEEE/CVF conference on computer vision and pattern recognition*. 10174–10183.
- [42] Yanlin Zhou, George Pu, Xiyao Ma, Xiaolin Li, and Dapeng Wu. 2020. Distilled one-shot federated learning. *arXiv preprint arXiv:2009.07999* (2020).
- [43] Zhuangdi Zhu, Junyuan Hong, and Jiayu Zhou. 2021. Data-free knowledge distillation for heterogeneous federated learning. In *International conference on*

A Visualization of Heterogeneous Federated Data Distributions

FL often encounters data heterogeneity, where client data distributions vary significantly. This heterogeneity is commonly modeled using the Dirichlet distribution with a concentration parameter α , which controls the degree of data imbalance among clients. Fig. 9 illustrates different levels of heterogeneous data distributions across clients for $\alpha = \{0.5, 0.3, 0.1, 0.01\}$. As α decreases, data partitions become more skewed, leading to higher heterogeneity. At $\alpha = 0.5$, data distribution is relatively balanced, whereas, at $\alpha = 0.01$, each client possesses highly imbalanced and disjoint subsets, exacerbating training challenges. Understanding the impact of data heterogeneity is crucial for designing robust FL algorithms. A lower α increases the difficulty of knowledge transfer across clients, making aggregation less effective, which highlights the importance of adaptive strategies like FedHydra to mitigate these challenges.

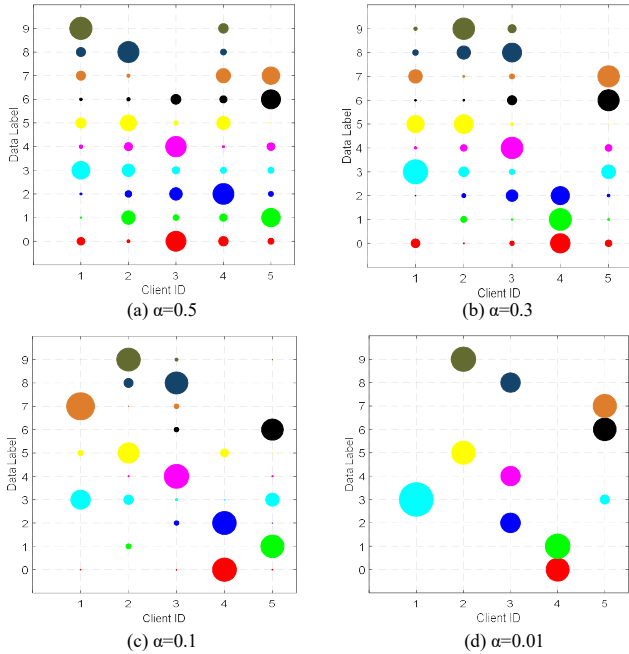


Figure 9: Visualization of heterogeneous distributions of client data characterized by four diverse α values, with MNIST used as an illustration. The horizontal axis denotes the client ID, while the vertical axis represents the class label. Each circle’s size corresponds to the number of data samples linked to a specific class, and circles of identical color denote the same class label.

B More Performance Overview Results on MNIST and SVHN

Fig. 10 shows the curves of accuracy versus distillation epoch over MNIST with $\alpha = \{0.5, 0.3, 0.1, 0.01\}$, the results show that FedHydra overtakes other baseline methods after round 15 epochs, and the proposed FedHydra fluctuates but still can reach the peak at 60 epochs

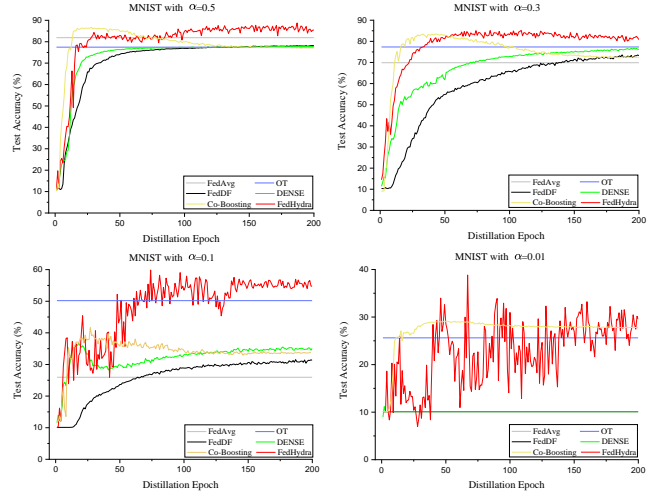


Figure 10: Test accuracy versus distillation epoch over MNIST with $\alpha = \{0.5, 0.3, 0.1, 0.01\}$.

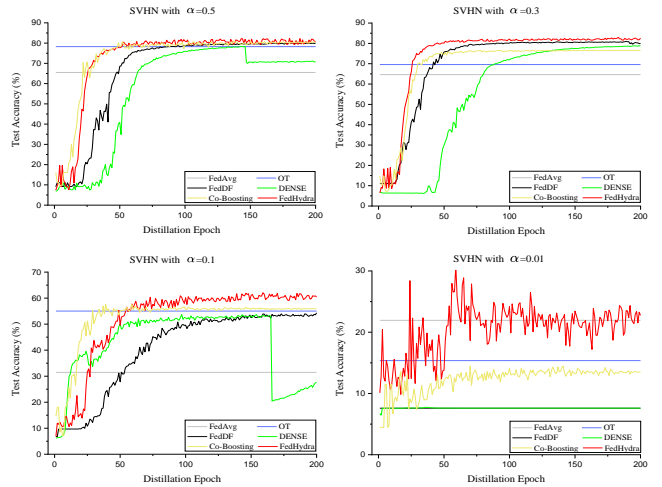


Figure 11: Test accuracy versus distillation epoch over SVHN with $\alpha = \{0.5, 0.3, 0.1, 0.01\}$.

around 35.00% when $\alpha = 0.01$, while others keep the performances as 10%.

On the SVHN dataset, FedHydra outperforms other baseline methods after 50 epochs as shown in Fig. 11. Additionally, FedHydra shows a dithering upward trend and peaks around 60 epochs when $\alpha = 0.01$.

C Extended Analysis

C.1 Impact of Client Numbers

Furthermore, we also test the impact of client numbers on CIFAR10 by varying the numbers of clients $K = \{5, 10, 20, 50, 100\}$, as shown in Table 7. All the methods decrease when the client number increases. However, FedHydra has less impact than other methods, FedHydra achieves 47.40% when $K = 100$ and outperforms the

second-best DENSE with only 36.25%. Thanks to the proposed SA algorithm, FedHydra minimally affects the increase in clients.

Table 7: Top-1 test accuracy achieved by FedAvg, OT, FedDF, DENSE, Co-Boosting, and FedHydra over CIFAR10 with different client numbers $K = \{5, 10, 20, 50, 100\}$.

Client K	FedAvg	OT	FedDF	DENSE	Co-Boosting	FedHydra
5	38.26	52.88	54.81	58.48	62.88	63.15
10	41.71	47.86	50.17	55.43	61.56	61.58
20	33.47	44.26	38.70	42.50	53.49	59.64
50	31.75	40.37	37.85	39.09	45.21	52.66
100	27.23	37.18	33.90	36.25	38.96	47.40

C.2 Performance Under Multiple Global Training Rounds

We extend our experiments to multiple global rounds. Specifically, we fix the local epoch $E = 50$ and $\alpha = 0.1$ to evaluate the performance of diverse methods on CIFAR10 with varying client distributions. Table 8 summarizes the relevant evaluation results. The results in Table 8 show that FedHydra outperforms the other methods with different global training rounds from $T = \{1, 2, 3, 4, 5\}$. FedHydra steadily increases and reaches a peak when $T = 3$, which outperforms DENSE by 1.86%.

Table 8: Top-1 test accuracy achieved by FedAvg, OT, FedDF, DENSE, Co-Boosting, and FedHydra over SVHN with $\alpha = 0.1$ under multiple global rounds.

Global round	FedAvg	OT	FedDF	DENSE	Co-Boosting	FedHydra
$T=1$	28.31	41.85	48.13	48.22	46.87	53.27
$T=2$	34.55	44.32	56.62	54.67	57.24	59.98
$T=3$	44.60	52.29	65.61	68.44	65.14	70.30
$T=4$	57.05	53.96	63.62	66.83	63.59	68.58
$T=5$	61.59	64.01	66.66	64.57	64.07	70.39

C.3 Visualization of Synthetic Data

To assess how synthetic data compares to actual training data, we provide the image comparison between the original training data and synthetic data on FashionMNIST and CIFAR-10 in Fig. 12. The figure demonstrates that the first and third rows display the original data from FashionMNIST and CIFAR10, respectively. In contrast, the second and last rows showcase the synthetic data produced by models trained on the FashionMNIST and CIFAR-10 datasets. Notably, the synthetic data differ significantly from the original data, effectively minimizing the risk of exposing sensitive client information. Despite the marked visual differences, the synthetic data contribute to our method outperforming other baseline approaches in performance. This highlights that synthetic data should ideally be easily distinguishable from real data while supporting superior model training outcomes.

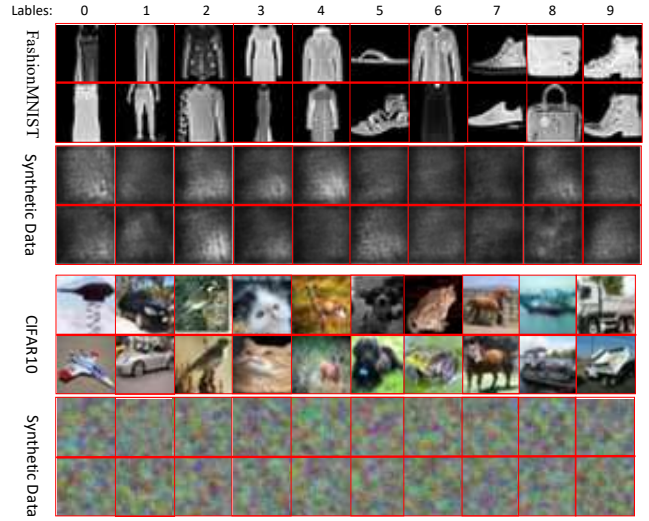


Figure 12: Visualization of synthetic data generated by the generator about FashionMNIST and CIFAR10.

D More Experiment Results on SVHN under OSFL Model Heterogeneity

Table 9 presents the top-1 test accuracy on SVHN under both data and model heterogeneity, where five different client models (GoogleNet, ResNet18, two custom CNNs, and LeNet) are used, with ResNet18 as the server model. As α decreases, data heterogeneity increases, leading to performance degradation across all methods. At $\alpha = 0.01$, FedDF and DENSE drop to 43.82% and 42.39%, respectively, while FedHydra maintains the highest accuracy of 54.33%, demonstrating its robustness. Co-Boosting performs better than FedDF and DENSE but remains lower than FedHydra. For moderate heterogeneity ($\alpha = 0.3, 0.5$), all methods perform better, with FedDF and DENSE reaching 77.22% and 75.75% at $\alpha = 0.3$, but FedHydra still achieves the highest accuracy at 77.52%. As heterogeneity decreases ($\alpha = 0.5$), performance stabilizes across all methods, but FedHydra maintains a slight edge. These results confirm that FedHydra is more resilient to both data and model heterogeneity, consistently outperforming baseline methods, particularly under extreme heterogeneity ($\alpha = 0.01$).

Table 9: Top-1 test accuracy achieved by FedDF, DENSE, Co-Boosting, and FedHydra over SVHN with personalized client models. M1 to M5 represent different neural network architectures: GoogleNet, ResNet18, two custom CNN models, and LeNet, respectively.

α	Personalized Client Model					Server (ResNet18)			
	M1	M2	M3	M4	M5	FedDF	DENSE	Co-Boosting	FedHydra
$\alpha=0.01$	24.17	7.59	29.81	34.76	19.52	43.82	42.39	45.72	54.33
$\alpha=0.1$	42.28	14.84	39.64	34.80	31.17	37.43	36.00	44.25	47.45
$\alpha=0.3$	66.78	65.62	38.22	58.73	64.19	77.22	75.75	73.21	77.52
$\alpha=0.5$	72.54	70.72	39.74	69.24	64.56	69.75	64.67	69.93	71.29

Table 10 presents the top-1 test accuracy on SVHN and CIFAR10 under the 2c/c setting in heterogeneous OSFL, where five different client models (GoogleNet, ResNet18, two custom CNNs, and

Table 10: Top-1 test accuracy achieved by FedDF, DENSE, Co-Boosting, and FedHydra over SVHN and CIFAR10 with 2c/c in heterogeneous OSFL. M1 to M5 represent different neural network architectures: GoogleNet, ResNet18, two custom CNN models, and LeNet, respectively.

Dataset with 2c/c	Personalized Client Model					Server (ResNet18)			
	M1	M2	M3	M4	M5	FedDF	DENSE	Co-Boosting	FedHydra
SVHN	25.78	26.30	18.48	15.13	11.85	24.72	20.42	27.34	31.22
CIFAR10	19.43	18.10	18.69	19.62	19.00	31.05	26.18	33.54	38.57

LeNet) are used, with ResNet18 as the server model. For SVHN, all methods experience performance degradation due to extreme data heterogeneity. FedDF and DENSE achieve 24.72 and 20.42, respectively, while Co-Boosting improves to 27.34. FedHydra maintains the highest accuracy at 31.22, demonstrating its robustness. On CIFAR10, the trend remains similar. DENSE and FedDF obtain 26.18 and 31.05, while Co-Boosting slightly improves to 33.54. FedHydra achieves the best performance at 38.57, showing its effectiveness in handling both model and data heterogeneity. These results indicate that FedHydra consistently outperforms other methods under the challenging 2c/c setting, demonstrating better adaptability to heterogeneous federated learning scenarios.

E More Experiment Results Under Multiple Global Rounds Across Diverse α Values

Table 11, 12, 13, 14, 15, 16, 17 and 18 provide the relevant test results with $\alpha = \{0.5, 0.3, 0.01\}$ and 2c/c under five global rounds.

Table 11: Top-1 test accuracy achieved by FedAvg, OT, FedDF, DENSE, Co-Boosting, and FedHydra over SVHN with $\alpha = 0.5$ under multiple global rounds.

Global round	FedAvg	OT	FedDF	DENSE	Co-Boosting	FedHydra
T=1	58.88	60.32	80.55	79.50	82.66	84.97
T=2	71.36	69.83	84.22	82.88	82.93	85.37
T=3	85.73	78.12	85.76	84.21	85.07	86.41
T=4	84.12	80.95	85.04	83.53	85.66	86.46
T=5	83.84	82.12	85.20	84.60	85.98	86.81

Table 12: Top-1 test accuracy achieved by FedAvg, OT, FedDF, DENSE, Co-Boosting, and FedHydra over CIFAR10 with $\alpha = 0.5$ under multiple global rounds.

Global round	FedAvg	OT	FedDF	DENSE	Co-Boosting	FedHydra
T=1	38.26	47.56	48.14	50.23	50.68	53.48
T=2	41.71	48.93	49.26	52.58	55.21	57.09
T=3	45.42	50.33	48.71	55.39	57.20	62.75
T=4	49.81	53.61	48.86	53.81	57.66	61.83
T=5	51.75	53.80	49.70	53.49	58.72	64.71

Table 11 and 12 shows that the proposed FedHydra outperforms and is more stabilized than all the other methods from different global rounds when $\alpha = 0.5$. The performance of FedHydra keeps above 80% on SVHN and outperforms the best second method 2% to

3%. The gap is much higher on CIFAR-10, where FedHydra can outperform more than 10%, compared with the second-best DENSE on the 5th global round. Table 13 and 14 present that FedHydra consistently outperforms the other methods on both datasets, demonstrating a marked advantage, particularly on the more complex CIFAR10 dataset. For instance, it peaks at 86.72% on SVHN and 58.43% on CIFAR-10, significantly higher than its competitors. The α is set to 0.01 on Table 14, FedHydra consistently outperforms the other algorithms across all rounds and both datasets, demonstrating exceptional adaptability and robustness under high data heterogeneity. Specifically, FedHydra’s accuracy peaks at 39.58% on SVHN and 39.76% on CIFAR10, significantly surpassing the next-best results from other models.

Table 13: Top-1 test accuracy achieved by FedAvg, OT, FedDF, DENSE, Co-Boosting, and FedHydra over SVHN with $\alpha = 0.3$ under multiple global rounds.

Global round	FedAvg	OT	FedDF	DENSE	Co-Boosting	FedHydra
T=1	61.17	73.55	77.99	76.76	78.60	79.14
T=2	73.50	75.99	84.21	82.68	80.46	84.83
T=3	84.29	78.36	84.49	84.81	83.22	85.56
T=4	84.13	75.48	85.04	83.82	84.05	86.02
T=5	84.96	77.59	85.89	84.62	84.71	86.72

Table 14: Top-1 test accuracy achieved by FedAvg, OT, FedDF, DENSE, Co-Boosting, and FedHydra over CIFAR10 with $\alpha = 0.3$ under multiple global rounds.

Global round	FedAvg	OT	FedDF	DENSE	Co-Boosting	FedHydra
T=1	33.72	36.56	37.56	41.54	48.01	50.01
T=2	37.56	39.62	38.94	46.44	52.30	57.00
T=3	36.04	38.24	40.73	47.10	56.06	58.18
T=4	41.73	43.00	41.10	46.20	55.21	58.43
T=5	44.26	46.85	41.03	48.55	51.34	55.97

Tables 15 and 16 present the top-1 test accuracy on SVHN and CIFAR10 under extreme data heterogeneity ($\alpha = 0.01$) across different global training rounds. For SVHN, most methods show inconsistent performance across rounds due to the severe heterogeneity. FedDF remains at 7.59 across all rounds, indicating poor adaptation. FedHydra achieves the highest accuracy at each round and significantly improves at $T = 5$ with 39.58, demonstrating its robustness in handling extreme non-IID settings. Co-Boosting maintains relatively stable performance but falls behind FedHydra, while FedAvg and OT show fluctuations. For CIFAR10, FedHydra consistently outperforms other methods across all rounds. The performance of FedDF remains low, while FedAvg and OT show gradual improvements. Co-Boosting performs well but does not surpass FedHydra. Notably, FedHydra achieves its highest accuracy of 39.76 at $T = 3$, maintaining strong performance across later rounds.

Table 17 and 18 assesses the performance under a 2c/c setting across five global training rounds. FedHydra consistently outshines the other algorithms in both datasets, showing its superior adaptability and robustness, with peak accuracies reaching 65.76% on

SVHN and 38.76% on CIFAR10 by the fifth round. FedDF generally performs well on SVHN, albeit less consistently on CIFAR10, while DENSE exhibits mixed results across rounds and datasets. FedAvg consistently underperforms, highlighting its limitations in more complex or skewed data environments. Overall, FedHydra emerges as the most effective method, particularly adept at handling challenges presented by the $2c/c$ setting, suggesting strong capabilities in managing diverse and complex data distributions in federated learning scenarios. These results underscore FedHydra’s potential effectiveness in federated learning scenarios where managing diverse data distributions is critical, marking it as a superior choice in handling complex data heterogeneity challenges in federated environments.

Table 15: Top-1 test accuracy achieved by FedAvg, OT, FedDF, DENSE, Co-Boosting, and FedHydra over SVHN with $\alpha = 0.01$ under multiple global rounds.

Global round	FedAvg	OT	FedDF	DENSE	Co-Boosting	FedHydra
T=1	19.60	23.68	7.59	7.59	25.63	29.58
T=2	20.10	24.01	7.59	7.59	25.04	27.75
T=3	19.58	26.34	7.59	19.77	28.19	31.73
T=4	28.58	29.88	7.59	9.86	28.05	30.98
T=5	21.73	27.56	7.59	8.04	26.99	39.58

Table 16: Top-1 test accuracy achieved by FedAvg, OT, FedDF, DENSE, Co-Boosting, and FedHydra over CIFAR10 with $\alpha = 0.01$ under multiple global rounds.

Global round	FedAvg	OT	FedDF	DENSE	Co-Boosting	FedHydra
T=1	10.00	16.12	14.39	23.84	26.60	30.13
T=2	17.77	20.33	14.89	24.84	29.88	37.67
T=3	26.02	25.98	16.42	27.24	33.68	39.76
T=4	25.57	29.50	16.79	29.16	34.07	38.17
T=5	27.68	26.38	17.59	26.04	35.12	38.30

Table 17: Top-1 test accuracy achieved by FedAvg, OT, FedDF, DENSE, Co-Boosting, and FedHydra over SVHN with $2c/c$ under multiple global rounds.

Global round	FedAvg	OT	FedDF	DENSE	Co-Boosting	FedHydra
T=1	26.40	31.33	24.51	35.57	41.56	49.30
T=2	36.37	38.66	36.00	29.54	46.33	57.35
T=3	30.00	45.38	54.43	43.53	53.04	62.45
T=4	39.56	44.02	58.41	38.65	50.34	59.58
T=5	34.53	42.13	57.12	34.52	55.86	65.76

F Time Complexity Analysis

Fig. 13 compares the running time of DENSE and FedHydra over multiple runs ($R = 1$ to $R = 5$). The y-axis represents the running time in seconds, while the x-axis denotes the number of runs. FedHydra consistently requires more computation time than DENSE across all runs. As R increases, both methods show a gradual rise in running time. At $R = 5$, FedHydra reaches approximately 5690

Table 18: Top-1 test accuracy achieved by FedAvg, OT, FedDF, DENSE, Co-Boosting, and FedHydra over CIFAR10 with $2c/c$ under multiple global rounds.

Global round	FedAvg	OT	FedDF	DENSE	Co-Boosting	FedHydra
T=1	12.23	13.86	17.84	23.57	27.78	28.34
T=2	15.62	15.33	18.61	22.05	22.66	25.54
T=3	16.10	18.66	16.76	25.97	29.00	32.25
T=4	20.44	22.36	15.81	20.06	34.11	35.69
T=5	18.24	21.02	17.28	24.24	34.88	38.76

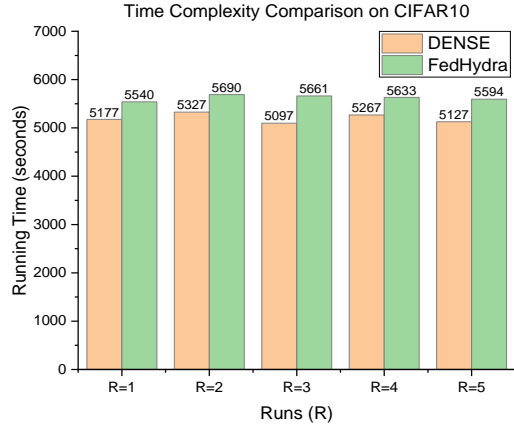


Figure 13: Time complexity comparison of FedHydra and DENSE based on five repeated runs (seconds).

seconds, whereas DENSE remains lower at 5540 seconds. The gap between the two remains stable, indicating that FedHydra incurs a higher computational cost while maintaining its superior performance. These results highlight the trade-off between accuracy and efficiency, as FedHydra achieves better performance at the cost of increased computational overhead.

G Details of Client Models

GoogleNet is a deep convolutional neural network known for its Inception modules, which extract multi-scale spatial features efficiently. It combines parallel 1×1 , 3×3 , and 5×5 convolutions, along with max pooling, within a single module to capture features of varying sizes. The network reduces computational complexity using 1×1 convolutions for dimensionality reduction and auxiliary classifiers to combat vanishing gradients. With 22 layers, GoogleNet demonstrated state-of-the-art performance on image recognition tasks while being computationally efficient.

ResNet-18 features skip connections to address vanishing gradient problems in deep networks. It uses residual blocks, where identity mappings allow gradients to flow through bypassed layers, enabling effective training of deeper architectures. With 18 layers, ResNet-18 balances depth and computational efficiency, making it versatile for tasks like image recognition, object detection, and feature extraction in moderately complex scenarios.

A basic CNN typically consists of two to three convolutional layers with ReLU activation, followed by max pooling layers and fully

connected layers for classification. These architectures are straightforward, often starting with 32 filters and increasing depth gradually. Designed for entry-level image datasets like MNIST or CIFAR-10, these networks are flexible and serve as an excellent starting point for learning about convolutional neural networks. A slightly deeper variant might incorporate more layers, batch normalization, or larger filter counts for more complex tasks.

LeNet is a pioneering CNN designed for digit recognition on datasets like MNIST. Its architecture includes two convolutional layers paired with average pooling, followed by two fully connected layers and a softmax output layer. As one of the first successful CNNs, LeNet laid the groundwork for modern convolutional networks by introducing key concepts like convolutional feature extraction and backpropagation-based training, making it historically significant in deep learning.

H Details of Dataset

The MNIST [16] dataset is a foundational resource in machine learning, specifically for computer vision tasks, consisting of 70,000 handwritten digit images used to train and test image recognition algorithms. It is divided into a training set of 60,000 examples and a test set of 10,000 examples, with each image being a 28x28 pixel grayscale representation of digits 0 through 9. MNIST serves as a benchmark for evaluating the performance of machine learning models. Despite its simplicity, MNIST is critically acclaimed for its role in advancing machine learning techniques.

Fashion-MNIST [36] is an advanced dataset introduced as an alternative to the original MNIST, aimed at providing a greater challenge for machine learning models in image classification. Developed by Zalando, it comprises 70,000 grayscale images of fashion items categorized into 10 types, such as T-shirts, trousers, and sneakers, divided into a training set of 60,000 and a test set of 10,000 images. Designed to be a direct replacement for MNIST, Fashion-MNIST maintains the same format and size, encouraging more sophisticated modeling techniques without requiring significant computational resources, thus making it suitable for benchmarking purposes.

The Street View House Numbers (SVHN) [25] dataset is a complex, real-world image dataset derived from Google Street View images, designed for machine learning tasks like digit recognition. It contains over 600,000 digit images, offering a substantial challenge due to its size and the real-life variability of its images, including differences in lighting, digit styles, and background clutter. SVHN is structured into two formats: the first includes full numbers with bounding boxes for digit localization, while the second focuses on images centered around single digits for classification tasks. This dataset is particularly valued for testing the robustness of machine learning models, such as convolutional neural networks, in recognizing numbers under varied and realistic conditions.

The CIFAR-10 [15] dataset, established by the Canadian Institute for Advanced Research, is a fundamental benchmark for machine learning and computer vision research, focusing on object recognition tasks. It comprises 60,000 color images of 32x32 pixels each, evenly distributed across 10 classes - airplanes, cars, birds, cats, deer, dogs, frogs, horses, ships, and trucks. With a division of 50,000 images for training and 10,000 for testing, CIFAR-10 challenges algorithms with its real-world variability, including diverse object orientations, varied backgrounds, and fluctuating lighting conditions.

This dataset represents a moderate step up in complexity from introductory datasets like MNIST, providing a balanced platform for testing and refining advanced image recognition models, especially convolutional neural networks, within a controlled yet realistic setting.